Effect of Pressure on the Mechanism of Hydrolysis of Maltoheptaose and Amylose Catalyzed by Porcine Pancreatic α-Amylase

Tadashi Matsumoto,[†] Syoichi Makimoto,[‡] and Yoshihiro Taniguchi*[,‡]

Industrial Research Center of Shiga Prefecture, 232 Kamitoyama, Ritto, Shiga 520-30, Japan, and Department of Chemistry, College of Science and Engineering, Ritsumeikan University, 1-1-1 Nojihigashi, Kusatsu, Shiga 525-77, Japan

Pressure effects over time on the products accompanying the hydrolysis of maltoheptaose (G7) and amylose catalyzed by porcine pancreatic α-amylase (PPA) were measured up to 300 MPa at 30 °C. Under moderate pressure up to 100 MPa, the initial rates of hydrolysis of G7 increased, and at the pressure range of 100−300 MPa, rates decreased gradually to produce maltose (G2), maltotriose (G3), maltotetraose (G4), and maltopentaose (G5). For amylose, the pressure dependence on the time course for G2, G3, and G4 is similar to that for G7. From the pressure dependence of the initial rates of hydrolysis of G7, the volume difference between enzyme−substrate (ES) complexes of G2 and G5 and the ES complex of G3 and G4 is 3.4 cm^3/mol. At the multiple attacked process of amylose, the volume differences of ES complexes are −6.3 cm^3/mol for G2 and G3, +4.8 cm^3/mol for G3 and G4, and −1.5 cm^3/mol for G2 and G4. These results suggest that pressure is a good tool to control the pathway of enzyme action of α-amylase and thus to produce the composition of products commercially desired.

Keywords: *Pressure; porcine pancreatic α-amylase; maltoheptaose; amylose; volume change*

INTRODUCTION

During the past few years, there have been published many interesting pressure effects on biological systems (Gross and Jaenicke; 1994, Mozhaev et al., 1994, 1996; Tausher, 1995). Especially, recent progress in research into the use of high-pressure techniques in food science and technology (Balny et al., 1992; Hayashi, 1992) has led to the manufacture of products at high pressure. In fact, some commercial jams had been sterilized using high pressure. This progress is due to the basic understanding of high-pressure effects on biological systems. We reported that there are two different kinds of high- and moderate-pressure effects on proteins, enzymes, and model systems (Suzuki and Taniguchi, 1972). The high-pressure region above about 300 MPa induces the denaturation of proteins and the inactivation of enzymes. On the other hand, the moderate-pressure region below about 300 MPa affects the acceleration of enzyme action and some exchange reactions of weak chemical interactions in an enzyme molecule itself and enzyme−substrate complexes. We have studied the effect of moderate pressure on the enzyme reactions and model systems (Taniguchi and Makimoto, 1988, 1996) and the hydrolysis catalyzed by serine protease (Taniguchi and Suzuki, 1980; Taniguchi and Makimoto, 1983; Makimoto et al., 1984, 1986, 1987, 1988; Seto et al., 1992), cyclodextrins (Taniguchi et al., 1981; Makimoto et al., 1982, 1984), and Taka-amylase (Makimoto et al., 1989). Pressure does change the specificity of enzymatic action (Makimoto et al., 1982, 1984; Makimoto and Taniguchi, 1987, 1988) and forms of some protease-catalyzed peptides (Kunugi et al., 1987). Therefore, it is expected that the moderate pressure can effectively amplify or control the molecular recognition of substrate molecules and the specificity of the enzymatic action. Application of these pressure effects on biological systems in food science and technology allows discovery of new functional and variable food materials commercially desired.

Porcine pancreatic α-amylase (EC 3.2.1.1; PPA) is a typical endoamylase used to catalyze the hydrolysis of α-D-(1,4) glucoside bonds in starch components, glycogen, and various oligosaccharides. PPA consists of a single polypeptide chain of 496 amino acid residues of known sequence with a molecular mass of 55 000 Da and optimum pH of 6.9 (Sakano et al., 1983; Pasero et al., 1986). From kinetic studies, it is suggested that the active site of PPA is composed of five binding subsites per glucose unit, and glucoside bonds of substrates are hydrolyzed between subsites 2 and 3, numbered from the subsite proximal to the reducing end of the substrate as shown in Figure 1 (Robyt and French, 1970, 1980; Probanov et al., 1984). Therefore, the composition of hydrolysate depends on the occupancy of the enzyme subsite by substrate in the productive binding mode. Published research has illustrated the effect of chemical modifications of the enzyme (Ishikawa and Hirata, 1989; Yamashita et al., 1991), modified substrates (Chan et al., 1984; Braun et al., 1985a−c), substrate analogs (Kondo et al., 1990), or pH (Ishikawa et al., 1990, 1991) on the action pattern or binding mode with substrates of PPA.

Previously, we studied the effect of pressure on the mechanism of hydrolysis of maltooligosaccharides, maltotetraose (G4) maltopentaose (G5), and maltohexaose (G6) catalyzed by PPA, and found that pressure can change the composition of products of hydrolysis of G6 but not the composition of hydrolyzed products of G4 and G5 (Matsumoto et al., 1997). To evaluate the phenomena of the pressure effects on catalytic sites depending on the chain length of oligosaccharides, we extend similar studies about the pressure effects on the hydrolase-catalyzed degradation of higher polymerized

* Author to whom correspondence should be addressed [telephone +81 (775) 61-2785; fax +81 (775) 61-2659; e-mail taniguti@bkc.ritsumei.ac.jp].

[†] Industrial Research Center of Shiga Prefecture.

[‡] Ritsumeikan University.

S0021-8561(97)00137-4 CCC: $14.00

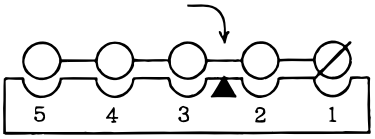

Figure 1. Schematic drawing of subsite structure of the PPA−G5 substrate complex.

oligosaccharide, G7 and amylose, to gain understanding of the mechanism of multiple attack of degradation.

MATERIALS AND METHODS

Materials. PPA (twice crystallized) was purchased from Sigma Chemical Co. (St. Louis, MO), maltoheptaose (biochemical grade) from Wako Pure Chemicals Co. (Osaka, Japan), and enzymatically synthesized linear amylose (molecular mass 1 000 000 Da) from Ajinoki Co. (Aichi, Japan). All biochemicals were used without further purification. Other chemicals were of commercial guaranteed grade.

High-Pressure Time Course Studies. PPA was diluted with 50 mM *N*-tris[hydroxymethyl]methyl-2-aminoethanesulfonic acid (TES) buffer, pH 6.9, containing 25 mM sodium chloride to 9.1 nM. Maltoheptaose was dissolved in the same buffer to 17.4 mM at room temperature, and amylose was dissolved in buffer solution by heat treatment at 100 °C for 5 min to 10 μM. After the PPA and substrate solutions were mixed, each enzyme concentration was 2.3 nM for G7 and amylose.

Hydrolysis was performed as follows. After 1 mL of the enzyme solution and 3 mL of the substrate solution were mixed quickly, the mixture was enclosed in a polyethylene container (4 mL). As soon as the container was inserted in a high-pressure apparatus (Mitsubishi Heavy Industry Co. MFP-7000, Hiroshima, Japan) thermostated at 30 ± 0.2 °C, pressure was applied. The temperature of the container was monitored by the thermistor. It takes 1 min (on average) for a compression up to a desired experimental pressure after an enzyme and a substrate solution are mixed. The reaction was carried out for an appropriate time (100 min), and then the container was taken out as quickly as possible. After that, 0.1 mL of 20% sulfosalicylic acid was added to stop the enzyme reaction.

HPLC Analysis. To remove the enzyme protein and higher molecular weight maltosaccharides, an aliquot of the reaction mixture was filtered through the ultrafiltration membrane with cutoff molecular mass 10 000 Da (polyethersulfon membrane). Maltooligosaccharides in the hydrolysate were determined by a high-performance liquid chromatograph (Waters Co., LC module 1, Milford, MA) with a Polyamine II column (YMC Co., Kyoto, Japan), with length, diameter, particle size, and pore size of 250 mm, 4.6 mm, 5 μm, and 12 nm, respectively. The solvent used was acetonitrile/water (55:45). The flow rate was 0.8 mL/min, and the column temperature was 30 °C. Effluent was monitored with a differential refractometer (Waters Co., 410). The initial hydrolysis rates for G7 and amylose were determined by the nonlinear least-squares method with Taylor expansion equation from the time course.

RESULTS AND DISCUSSION

Maltoheptaose Substrate. The time course of G2, G3, G4, and G5 hydrolysates of maltoheptaose catalyzed by PPA was measured at four pressures, 0.1, 100, 200, and 300 MPa, respectively, and is shown in Figure 2. The initial rates for product formation are summarized in Table 1. Pressure up to 100 MPa accelerated the initial rates, and at the pressure range of 200−300 MPa the rates decreased gradually. This tendency is possibly due to the partial pressure-induced inactivation of enzyme (T. Matsumoto, S. Makimoto, and Y. Taniguchi, unpublished results, 1997). With increasing pressure, the ratio of produced composition of G4 to G2 increased. Pressure effects on the produced composition were

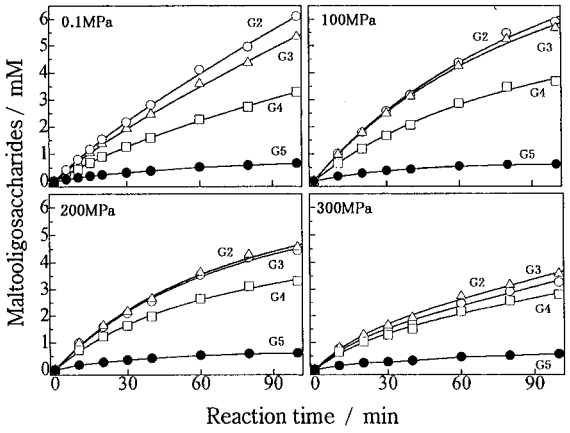

Figure 2. Time course of G2, G3, G4, and G5 products of G7 substrate catalyzed by PPA at 0.1, 100, 200, and 300 MPa and 30 °C. The final substrate and enzyme concentrations were 13 mM and 2.3 nM in 50 mM TES buffer, pH 6.9, containing 25 mM sodium chloride. Maltooligosaccharides were determined by HPLC. ○, G2; △, G3; □, G4; ●, G5.

Table 1. Initial Rates of Formation of G2, G3, and G4 from Hydrolysis of G7 Catalyzed by PPA

	pressure			
	0.1 MPa	100 MPa	200 MPa	300 MPa
v_{G2}[a]/μM min^{-1}	78	96	82	56
v_{G3}[b]/μM min^{-1}	69	94	85	62
v_{G4}[c]/μM min^{-1}	46	64	63	49
v_{G5}[d]/μM min^{-1}	13	15	13	9
$v_{G2} + v_{G4}$/μM min^{-1}	124	160	145	105
$1.72v_{G4}/v_{G2}$ (=K)	1.01	1.15	1.32	1.51

[a] $v_{G2} = d[G2]dt$. [b] $v_{G3} = d[G3]/dt$. [c] $v_{G4} = d[G4]/dt$. [d] $v_{G5} = d[G5]/dt$.

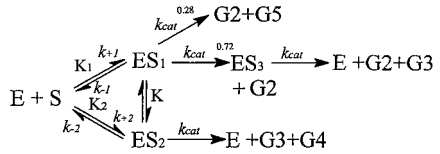

Figure 3. Reaction mechanism of hydrolysis of G7 catalyzed by PPA.

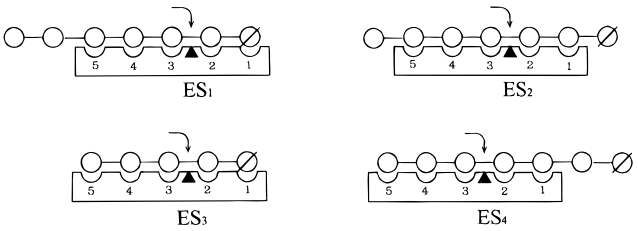

Figure 4. Schematic drawing of ES complexes and another possibly stable ES_4 complex of PPA with G7 substrate.

similar to those of hydrolysis of G6 substrate (Matsumoto et al., 1997).

From the distribution of products and structure of subsite of PPA, G7 was considered to be hydrolyzed through the pathway as shown in Figure 3. The binding models of enzyme and G7 including the possibly stable ES_4 complex are presented in Figure 4. The primary pathway takes a route to produce G2 and G5 through the ES_1 complex. At the first step of degradation, all G2 and 28% of G5 are removed from the binding site and about 72% of G5 still binds to the catalytic site to form ES_3 complex, which finally decomposes into G2 and G3 through the multiple attack. This ratio is consistent with the experimental results at each pressure from 0.1

to 300 MPa; the initial rate for the formation of G5 product corresponds to 16% of the initial rate for G2 described in Table 1. That is, at the steady state kinetics of the hydrolase-catalyzed degradation of G7, ES_3 is produced by 0.72 factor of ES_1. Both G2 and G3 are produced whenever ES_1 changes into ES_3 and G2. The secondary pathway is the hydrolysis to G3 and G4 after the formation of PPA and ES_2 complex. In this case, G3 and G4 remove easily from the binding site of α-amylase without the multiple attack. As the degree of polymerization of G4 is less than the subsite of PPA, the dissociation constant of PPA and G4 complex is expected to be large. There is the third possibility of a pathway to produce G3 and G4 after ES_4 complex formation as shown in Figure 4. However, in this experiment without ^{14}C-labeled G7, we cannot distinguish the third pathway from the secondary one, so we counted it as one part of the secondary pathway. The steady state condition is established during the time course of enzyme reaction under the condition of $[S]_0 = 13\ mM \gg [E]_0 = 2.3\ nM$.

Applying this hydrolysis of G7 to the steady state kinetics, the initial rates for G2, G3, and G4 are given by

$$v_{G2} = 1.72k_{cat}(K_{mapp}/K_{m1})[E]_0[S]/(K_{mapp} + [S]) \quad (1)$$

$$v_{G3} = k_{cat}(0.72K_{mapp}/K_{m1} + K_{mapp}/K_{m2})[E]_0[S]/(K_{mapp} + [S]) \quad (2)$$

$$v_{G4} = k_{cat}(K_{mapp}/K_{m2})[E]_0[S]/(K_{mapp} + [S]) \quad (3)$$

where K_{mapp} is the apparent Michaelis constant of the reaction. K_{m1} and K_{m2} are the dissociation constants for ES_1 and ES_2. They are represented by

$$K_{mapp} = K_{m1}K_{m2}/(K_{m1} + 1.72K_{m2}) \quad (4)$$

$$K_{m1} = [E][S]/[ES_1] = (k_{-1} + k_{cat})/k_{+1} \quad (5)$$

$$K_{m2} = [E][S]/[ES_2] = (k_{-2} + k_{cat})/k_{+2} \quad (6)$$

On the basis of subsite theory (Hiromi, 1970, 1985; Hiromi et al., 1983), it is assumed that each step for the hydrolysis is the same k_{cat} independent of binding modes of ES complexes. From the pressure dependence on the rates of hydrolysis under the condition of $K_m \ll [S]$, eqs 1 and 3 are rewritten

$$v_{G2} = 1.72k_{cat}(K_{mapp}/K_{m1})[E]_0 \quad (7)$$

$$v_{G4} = k_{cat}(K_{mapp}/K_{m2})[E]_0 \quad (8)$$

The sum of eqs 7 and 8 is a simple function of k_{cat} of $k_{cat}[E]_0$. The activation volume for this hydrolysis of G7 catalyzed by PPA is negative because both v_{G2} and v_{G4} increase at 100 MPa. At 200 and 300 MPa, the gradual decrease of v_{G2} and v_{G4} due to the partial pressure-induced inactivation overcomes the increasing rates of hydrolysis by pressure.

The pressure dependence of the composition of products and its pathway is discussed from the pressure dependence of equilibrium constants between ES_1 and ES_2, which are given by

$$1.72v_{G4}/v_{G2} = K_{m1}/K_{m2} = K \quad (9)$$

where the kinetic data up to 300 MPa are available

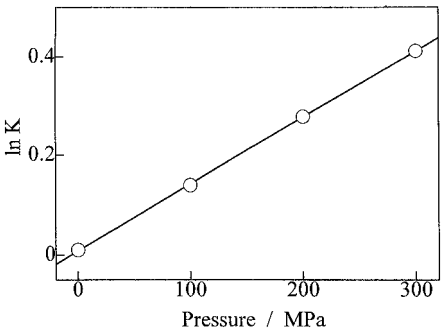

Figure 5. Pressure dependence of ln K for the hydrolysis of G7 catalyzed by PPA.

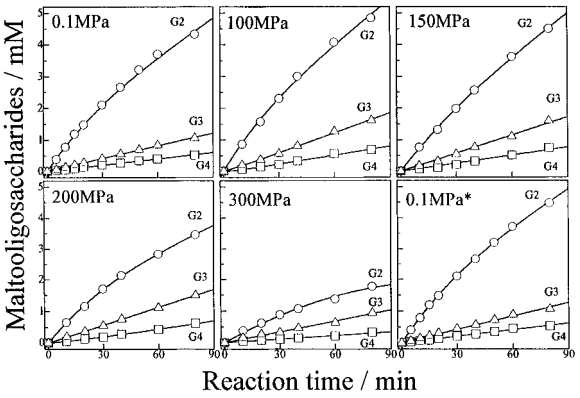

Figure 6. Time course of G2, G3, and G4 products of amylose catalyzed by PPA at 0.1, 100, 150, 200, and 300 MPa and 30 °C. The substrate and enzyme concentrations were 7.5 μM and 2.3 nM in 50 mM TES buffer, pH 6.9, containing 25 mM sodium chloride. Maltooligosaccharides were determined by HPLC. 0.1 MPa* is the time course of products for the hydrolysis catalyzed by PPA, which was treated for 90 min at 300 MPa and 30 °C. ○, G2; △, G3; □, G4.

because the pressure-induced inactivation of α-amylase is completely reversible. The obtained equilibrium constants are summarized in Table 1. They increased with increasing pressure. Pressure accelerated the reaction rate of the pathway through ES_2 complex and decelerated the pathway through ES_1. As a result, under pressure G4 increased and G2 decreased. As the pressure dependence of equilibrium constants gives information about the volume difference of partial molar volumes between ES_1 (V_{ES1}) and ES_2 (V_{ES2}), it is understood that V_{ES2} is smaller than V_{ES1} from this experiment. The difference of partial molar volumes between ES complexes, given by

$$V(ES_2) - V(ES_1) = \Delta V = -RT(\partial \ln K/\partial p)_T \quad (10)$$

from the pressure dependence of ln K as shown in Figure 5, is about $-3.4\ cm^3/mol$. At G6, the volume change for the formation of ES complex through the pathway to produce G3 from the degradation at the reducing end of G6 is smaller than that of ES complex formation through the G2 productive pathway. The volume change is about $-5.4\ cm^3/mol$ (Matsumoto et al., 1997). The absolute observed volume difference for G7 is a little bit smaller than that of G6 substrate. This is due to the former pathway containing the latter pathway to be explained later.

Amylose Substrate. The time course of the products of hydrolase-catalyzed degradation of amylose at various pressures is shown in Figure 6, and the initial rates for the product formation are summarized in Table 2. Pressure up to 100 MPa accelerated the initial rates,

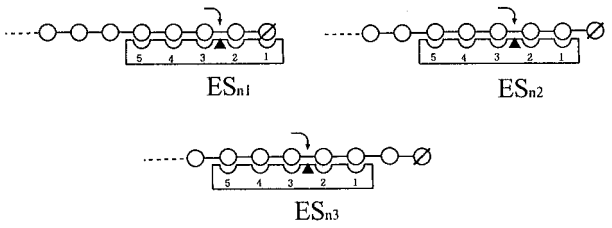

Figure 7. Schematic drawing of the two kinds of ES complexes between PPA and amylose through the multiple attack.

Table 2. Initial Rates of Formation of G2, G3, and G4 from Hydrolysis of Amylose Catalyzed by PPA

	pressure				
	0.1 MPa	100 MPa	150 MPa	200 MPa	300 MPa
ν_{G2}[a]/μM min^{-1}	81	88	72	63	33
ν_{G3}[b]/μM min^{-1}	14	20	19	19	12
ν_{G4}[c]/μM min^{-1}	6.6	7.4	6.3	5.6	3.2
$\nu_{G2} + \nu_{G3} + \nu_{G4}$/ μM min^{-1}	102	115	97	88	48
ν_{G3}/ν_{G2} (=K_{12})	0.17	0.23	0.26	0.30	0.36
ν_{G4}/ν_{G3} (=K_{23})	0.47	0.37	0.33	0.29	0.27
ν_{G4}/ν_{G2} (=K_{13})	0.081	0.084	0.088	0.089	0.097

[a] ν_{G2} = d[G2]/dt. [b] ν_{G3} = d[G3]/dt. [c] ν_{G4} = d[G4]/dt.

and at the pressure above 150 MPa, the rates decreased gradually. The decrement of rates of hydrolysis of amylose above 150 MPa is associated with the partially reversible pressure-induced inactivation. As shown at 0.1 MPa* in Figure 6, the time course of products for the hydrolysis-catalyzed by PPA, which was treated for 90 min at 300 MPa and 30 °C, agreed completely with the original one at 0.1 MPa and 30 °C. The increment of rates of hydrolysis under pressure suggested that the activation volumes for the hydrolysis catalyzed by PPA are negative. With increasing pressure, the ratio of the rates of G3 and G4 to G2 increased and the ratio of G4 to G3 decreased. This tendency of pressure effects on the rates and the composition of products is similar to that seen for G7 substrate. The reason pressure changed the ratio of the products' rates can be explained as follows. It is well-known that PPA hydrolysis took place through not only random attack but also multiple attack. The mechanism of multiple attack implies that in the process of the ES complex formation, enzyme can successively cleave the substrate molecules several times before the ES complex dissociates. PPA produces the lower polymerized oligosaccharides and behaves like an exo-amylase. We got lower polymerized oligosaccharides of G2, G3, and G4 but no higher polymerized ones above G5. Therefore, the PPA-catalyzed hydrolysis of amylose follows the multiple-attack mechanism. On the process of hydrolysis of amylose through multiple attack, three kinds of energetically stable ES complexes to produce G2, G3, and G4 are shown in Figure 7. At 0.1 MPa, the equilibrium state among the above three products is established. The free energy for the complex formation is lower, and the amount of products becomes larger. If there are volume differences among ES complexes, the larger amount of products with the smaller partial molar volume of ES complexes can be induced by pressure (Le Chatelier principle). To confirm this, we determined the volume changes accompanying ES complex formation from the pressure dependence of ln K according to the following method. The reaction scheme of PPA-catalyzed hydrolysis of amylose through multiple attack is presented in Figure 8. At first, amylose binds to the ambient active site of PPA to form

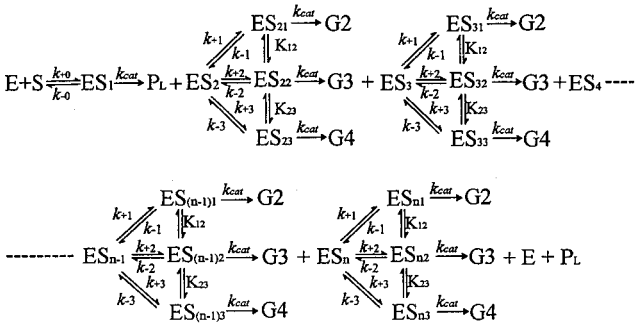

Figure 8. Reaction mechanism of hydrolysis of amylose catalyzed by PPA through multiple attack.

ES complexes, and then the complex is hydrolyzed into non-reducing-end oligosaccharides and reducing-end polymeric maltosaccharides. After the first step of hydrolysis, the former still exist on the active site of ES_2 and the latter is removed from the ES complex. ES_2 is the nonproductive ES complex. As the ES_2 complex is unstable at the free energy level, ES_{21}, ES_{22}, and ES_{23} are produced as soon as ES_2 changes into the productive form, and equilibria among ES_{21}, ES_{22}, and ES_{23} are established immediately to produce G2, G3, and G4. At the next stage, ES_3 is equivalent with ES_2, followed a reaction similar to that of ES_2, and produced ES_{31}, ES_{32}, and ES_{33}. This process naturally was considered that each rate of hydrolysis of glucoside bond for each ES complex as the same form the substite theory (Hiromi, 1970, 1985; Hiromi et al., 1983). Finally, the multiple attack was over when hydrolysis took place for the nth repeat and substrates were removed from the active site of PPA. The multiple attack is established to be $n = 7$ for amylose catalyzed by PPA (Robyt and French, 1970; Robyt, 1989). Assuming the PPA-catalyzed hydrolysis of amylose followed the multiple attack on the basis of subsite theory, the reaction rates are given by

$$\nu_{G2} = (n-1)k_{cat}(K_{m'}/K_{m1})[E]_0[[S]/(K_{m0} + n[S]) \quad (11)$$

$$\nu_{G3} = (n-1)k_{cat}(K_{m'}/K_{m2})[E]_0[S]/(K_{m0} + n[S]) \quad (12)$$

$$\nu_{G4} = (n-1)k_{cat}(K_{m'}/K_{m3})[E]_0[S]/(K_{m0} + n[S]) \quad (13)$$

where

$$K_{m'} = K_{m1}K_{m2}K_{m3}/(K_{m1}K_{m2} + K_{m2}K_{m3} + K_{m3}K_{m1}) \quad (14)$$

$$K_{m0} = [E][S]/[ES_1] = (k_{-0} + k_{cat})/k_{+0} \quad (15)$$

$$K_{m1} = [ES_n]/[ES_{n1}] = (k_{-1} + k_{cat})/k_{+1} \quad (16)$$

$$K_{m2} = [ES_n]/[ES_{n2}] = (k_{-2} + k_{cat})/k_{+2} \quad (17)$$

$$K_{m3} = [ES_n]/[ES_{n3}] = (k_{-3} + k_{cat})/k_{+3} \quad (18)$$

The ratio of each rate to produce G2, G3, and G4 is represented by eqs 19−21, where K_{12}, K_{23}, and K_{13} are the corresponding equilibrium constants among ES complexes.

$$\nu_{G3}/\nu_{G2} = K_{m1}/K_{m2} = K_{12} \quad (19)$$

$$\nu_{G4}/\nu_{G3} = K_{m2}/K_{m3} = K_{23} \quad (20)$$

$$\nu_{G4}/\nu_{G2} = K_{m1}/K_{m3} = K_{13} \quad (21)$$

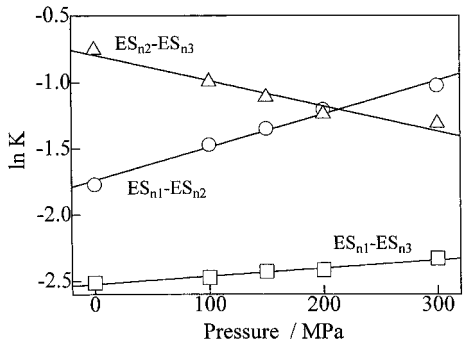

Figure 9. Pressure dependence of ln K_{12}, ln K_{23}, and ln K_{13}. ○, K_{12} ($ES_{n1} - ES_{n2}$); △, K_{23} ($ES_{n2} - ES_{n3}$); □, K_{13} ($ES_{n1} - ES_{n3}$).

The volumes among ES_{n1}, ES_{n2}, and ES_{n3} are estimated from eq 10 and the slope of plots of pressure vs ln K as shown in Figure 9 to be -6.3 cm^3/mol for K_{12}, $+4.8$ cm^3/mol for K_{23}, and -1.5 cm^3/mol for K_{13}, respectively. The order of partial molar volume is $V(ES_{n1}) > V(ES_{n3}) > V(ES_{n2})$. The volume change of -6.3 cm^3/mol for $K_{12} = [V(ES_{n2}) - V(ES_{n1})]$ is consistent with the difference of -6.3 cm^3/mol between $V(K_{23}) = [-1.5$ cm^3/mol $= V(ES_{n3}) - V(ES_{n2})]$ and $V(K_{13}) = [+4.8$ cm^3/mol $= V(ES_{n3}) - V(ES_{n1})]$. Previously (Matsumoto et al., 1997a), the volume changes between ES complexes could be explained by the formation of hydrogen bonds between OE2 of Glu-240 in PPA and a free glucose residue at the reducing end in the ES complex on the basis of the X-ray analysis data of PPA (Qian et al., 1993, 1994; Larson et al., 1994) and PPA−substrate complex (Casset et al., 1995). The fact that each ES complex showed the same nonreducing end in the long maltosaccharide chain could not explain the obtained volume differences among these ES complexes. Therefore, PPA-catalyzed hydrolysis of amylose would be explained by the above-described mechanism. When ES_{n1} substrate moves one glucose unit toward the reducing end to form ES_{n2}, the volume change decreased 6.3 cm^3/mol and increased 4.8 cm^3/mol after moving one more glucose unit toward the reducing end. This phenomenon is interesting and is explained by the formation of the hydrogen bonds between OE2 of Glu-240 of PPA at ES_{n2} complex, but at ES_{n3} the formation of a hydrogen bond between them is impossible because OH-1 of glucose is already formed with the glucose residue of the reducing end. In the case of G7, we already reported that the volume difference between ES_1 and ES_2 was 3.4 cm^3/mol for the ES_2 and ES_4 complexes. If the volume difference depends on the structure of the reducing end of ES complexes, the differences between ES_1 and ES_2 must be about 5−6 cm^3/mol and about 1−2 cm^3/mol for ES_1 and ES_4, so the average difference of about 3−4 cm^3/mol $[=[\Delta V(ES_2 - ES_1) + \Delta V(ES_4 - ES_1)]/2]$ is enough to satisfy the experimental values. These results suggest that pressure shows the possibility of control of the composition of products catalyzed by PPA and the design of the enzyme reaction when the volume differences among ES complexes are known.

ABBREVIATIONS USED

G2, maltose; G3, maltotriose; G4, maltotetraose; G5, maltopentaose; G7, maltoheptaose; PPA, porcine pancreatic α-amylase; TES, *N*-tris[hydroxymethyl]methyl-2-aminoethanesulfonic acid.

LITERATURE CITED

Balny, C., Hayashi, R., Heremans, K., Masson, P., Eds. *High Pressure and Biotechnology*; Colloque INSERM 224; John Libbey: London, 1992.

Braun, P. J.; French, D.; Robyt, J. F. The effect of substrate modification on porcine pancreatic α-amylase subsite binding: Hydrolysis of substrates containing 2-deoxy-D-glucose and 1-amino-2-deoxy-D-glucose. *Arch. Biochem. Biophys.* **1985a**, *242*, 231−239.

Braun, P. J.; French, D.; Robyt, J. F. The effect of substrate modification on binding of porcine pancreatic α-amylase: Hydrolysis of modified amylose containing D-allose residues. *Carbohydr. Res.* **1985b**, *141*, 265−271.

Braun, P. J.; French, D.; Robyt, J. F. Porcine pancreatic α-amylase hydrolysis of substrates containing 6-deoxy-D-glucose and 6-deoxy-6-fluoro-D-glucose and the specificity of substrate binding. *Carbohydr. Res.* **1985c**, *143*, 107−116.

Casset, R.; Imberty, A.; Haser, R.; Payan, F.; Perez, S. Molecular modelling of the interaction between the catalytic site of pig pancreatic α-amylase and amylose figments. *Eur. J. Biochem.* **1995**, *232*, 284−293.

Chan, Y. C.; Braun, P. J.; French, D.; Robyt, J. F. Porcine pancreatic α-amylase hydrolysis of hydroxyethylated amylose and specificity of subsite binding. *Biochemistry* **1984**, *23*, 5795−5800.

Gross, M.; Jaenicke, R. The influence of high hydrostatic pressure on structure, function and assembly of proteins and protein complexes. *Eur. J. Biochem.* **1994**, *221*, 617−630.

Hayashi, R., Ed. *High Pressure Biosciene and Food Science* (in Japanese); Sanei Shuppan: Kyoto, 1992.

Hiromi, K. Interpretation of dependency of rate parameters on the degree of polymation of substrate in enzyme-catalyzed reactions. Evaluation of substrate affinities of exo-enzyme. *Biochem. Biophys. Res. Commun.* **1970**, *40*, 1−6.

Hiromi, K. Principle and developments of the subsite theory with special reference to amylase-catalyzed reactions (in Japanese) *J. Jpn. Soc. Starch Sci.* **1985**, *32*, 84−93.

Hiromi, K.; Ohnishi, M.; Tanaka, A. Subsite structure and ligand binding mechanism of glucoamylase. *Mol. Cell. Biochem.* **1983**, *51*, 79−95.

Ishikawa, K.; Hirata, H. New substrate specificity of modified porcine pancreatic α-amylase. *Arch. Biochem. Biophys.* **1989**, *272*, 356−363.

Ishikawa, K.; Matsui, I.; Honda, K. Substrate-dependence shift of optimum pH in porcine pancreatic α-amylase-catalyzed reactions. *Biochemistry* **1990**, *29*, 7119−7123.

Ishikawa, K.; Matsui, I.; Honda, K.; Kobayashi, S.; Nakatani, H. The pH dependence of the action pattern in porcine pancreatic α-amylase catalyzed reaction for maltooligosaccharide substrate. *Arch. Biochem. Biophys.* **1991**, *289*, 124−129.

Kondo, H.; Nakatani, H.; Hiromi, K. Effect of maltotriitol on the action pattern of porcine pancreatic α-amylase using amylose as a substrate. *Carbohydr. Res.* **1990**, *206*, 161−166.

Kunugi, S.; Tanabe, K.; Fukuda, M.; Makimoto, S.; Taniguchi, Y. The effect of pressure on protease catalyzed peptide formation. *J. Chem. Soc., Chem. Commun.* **1987**, 1335−1336.

Larson, S. B.; Greenwood, A. G.; Cascio, D.; Day, J.; McPherson, A. Refined molecular structure of pig pancreatic α-amylase at 2.1 Å resolution. *J. Mol. Biol.* **1994**, *235*, 1560−1584.

Makimoto, S.; Taniguchi, Y. Effect of pressure on the presteady state kinetics of the hydrolysis of anilide substrates catalyzed by α-chymotrypsin. *Biochim. Biophys. Acta* **1987**, *914*, 304−307.

Makimoto, S.; Taniguchi, Y. Pressure effects on substrate activation phenomena in the α-chymotrypsin-catalyzed hydrolysis of *p*-nitrophenyl acetate. *Biochim. Biophys. Acta* **1988**, *954*, 343−346.

Makimoto, S.; Suzuki, K.; Taniguchi, Y. Pressure effect on the stereospecificity of the cleavage of phenyl acetates catalyzed by α-cyclodextrin. *J. Phys. Chem.* **1982**, *86*, 4544−4547.

Makimoto, S.; Suzuki, K.; Taniguchi, Y. Pressure dependence of the α-chymotrypsin catalyzed hydrolysis of amide and anilides. Evidence for the single proton-transfer mechanism. *J. Phys. Chem.* **1984**, *88*, 234−247.

Makimoto, S.; Suzuki, K.; Taniguchi, Y. Effects of pressure on the pre-steady-state kinetics of the hydrolysis of p-nitrophenyl pivalate catalyzed by α-chymotrypsin. *Bull. Chem. Soc. Jpn.* **1986**, *59*, 243−247.

Makimoto, S.; Nishida, H.; Taniguchi, Y. Pressure effects on thermal inactivation of Taka-amylase A. *Biochim. Biophys. Acta* **1989**, *996*, 233−239.

Matsumoto, T.; Makimoto, S.; Taniguchi, Y. Effect of pressure on the mechanism of hydrolysis of maltotetraose, maltopentaose, and maltohexaose catalyzed by porcine pancreatic α-amylase. *Biochim. Biophys. Acta* **1997**, in press.

Mozhaev, V. V.; Heremans, K.; Frank, J.; Masson, P.; Balny, C. Exploiting the effects of high hydrostatic pressure in biotechnological applications. *Trends Biotechnol.* **1994**, *2*, 493−501.

Mozhaev, V. V.; Heremans, K.; Frank, J.; Masson, P.; Balny, C. High pressure effects on protein structure and function. *Protein: Struct., Funct., Genet.* **1996**, *24*, 81−91.

Pasero, L.; Mazzei Pierron, Y.; Abadie, B.; Chicheportiche, Y.; Marchis Mouren, G. Subsite profile of the active center of porcine pancreatic α-amylase. Kinetic studies of maltooligosaccharides as substrates. *Biochim. Biophys. Acta* **1986**, *869*, 147−157.

Probanov, E.; Seinger, C.; Marchis-Mouren, G. Subsite profile of the active center porcine pancreatic α-amylase. Kinetic studies using maltooligosaccharides as substrate. *Biochem. Biophys. Res. Commun.* **1984**, *122*, 75−81.

Qian, M.; Haser, R.; Payan, F. Structure and molecular model refinement of pig pancreatic α-amylase at 2.1 Å resolution. *J. Mol. Biol.* **1993**, *231*, 785−799.

Qian, M.; Haser, R.; Buisson, G.; Duee, E.; Payan, F. The active center of a mammalian amylase. Structure of the complex of a pancreatic α-amylase with a carbohydrate inhibitor refined to 2.2 Å resolution. *Biochemistry* **1994**, *33*, 6284−6294.

Robyt, J. F. Mechanism and product specificity of α-amylases. *J. Jpn. Soc. Starch Sci.* **1989**, *36*, 287−301.

Robyt, J. F.; French, D. The action pattern of porcine pancreatic α-amylase in relationship to the substrate binding site in the enzyme. *J. Biol. Chem.* **1970**, *245*, 3917−3927.

Sakano, Y.; Takahashim, S.; Kobayashi, T. Purification and properties of two active components from crystalline preparation of porcine pancreatic α-amylase. *J. Jpn. Soc. Strach Sci.* **1983**, *30*, 30−37.

Seto, T.; Makimoto, S.; Mashimo, T.; Yoshiya, I.; Taniguchi, Y. Volatile anesthetics induced activation phenomena of α-chymotrypsin-catalyzed hydrolysis. *Biochim. Biophys. Acta* **1992**, *1116*, 204−209.

Suzuki, Y.; Taniguchi, Y. Effect of pressure on biopolymers and model systems. *Symp. Soc. Exp. Biol.* **1972**, *26*, 103−124.

Taniguchi, Y.; Suzuki, K. Pressure effects under pressure. IV. The hydrolysis of phenyl esters catalyzed by α-chymotrypsin up to 2000 bar. *Bull. Chem. Soc. Jpn.* **1980**, *53*, 1709−1713.

Taniguchi, Y.; Suzuki, K. Pressure inactivation of α-chymotrypsin. *J. Phys. Chem.* **1983**, *87*, 5185−5193.

Taniguchi, Y.; Makimoto, S. High pressure studies on enzyme reactions. *J. Mol. Catal.* **1988**, *47*, 323−334.

Taniguchi, Y.; Makimoto, S. Catalysis, polymeric (pressure effects). *Polymeric Materials Encyclopedia*; Salamone, J. C., Ed.; CRC Press: Boca Raton, FL, 1996; Vol. 2, pp 999−1003.

Taniguchi, Y.; Makimoto, S.; Suzuki, K. Pressure effects on the hydrolysis of p-nitrophenyl and 2-naphtyl acetate catalyzed by cyclodextrins. *J. Phys. Chem.* **1981**, *85*, 3469−3472.

Tauscher, B. Pasteurization of food by hydrostatic high pressure: chemical aspects. *Z. Lebensm Unters. Forsch.* **1995**, *200*, 3−13.

Yamashita, H.; Nakatani, H.; Tonomura, B. Substrate selective activation of histidine-modified porcine pancreatic α-amylase by chloride ion. *J. Biochem.* **1991**, *110*, 605−607.

Received for review February 18, 1997. Revised manuscript received June 17, 1997. Accepted June 26, 1997.[⊗] This work was supported by Grant for Industrial Research from the Shiga Prefecture, Japan.

JF970137H

[⊗] Abstract published in *Advance ACS Abstracts,* August 15, 1997.